

Electronic Supplementary Information

A Bayesian phase difference estimation: a general quantum algorithm for the direct calculation of energy gaps

Kenji Sugisaki,^{*abc} Chikako Sakai,^a Kazuo Toyota,^a Kazunobu Sato,^{*a} Daisuke Shiomi^a and
Takeji Takui^{*ad}

^a. *Department of Chemistry and Molecular Materials Science, Graduate School of Science, Osaka City University, 3-3-138 Sugimoto, Sumiyoshi-ku, Osaka 558-8585, Japan*

^b. *JST PRESTO, 4-1-8 Honcho, Kawaguchi, Saitama, 332-0012, Japan*

^c. *Centre for Quantum Engineering, Research and Education (CQuERE), TCG Centres for Research and Education in Science and Technology (TCG CREST), 16th Floor, Omega, BIPL Building, Blocks EP & GP, Sector V, Salt Lake, Kolkata 700091, India*

^d. *Research Support Department/University Research Administrator Centre, University Administration Division, Osaka City University, 3-3-138 Sugimoto, Sumiyoshi-ku, Osaka 558-8585, Japan*

Table of Contents

	Page
1. Definitions of quantum gates	S2
2. Computational conditions for quantum chemical calculations	S4
3. Quantum circuits for the state preparations and controlled-<i>Excit</i> operations	S14
4. Computational conditions for the numerical simulations of the BPDE algorithm	S17
5. Computational conditions for the numerical simulations of the BPE algorithm	S18
6. List of the calculated energies and energy gaps	S19
7. Trotter decomposition error analysis	S46
8. References	S48

1. Definitions of quantum gates

In quantum computers, qubits can be in an arbitrary superposition of the $|0\rangle$ and $|1\rangle$ states, as given in eqn (S1).

$$|\varphi\rangle = c_0|0\rangle + c_1|1\rangle \quad (\text{S1})$$

Here, c_0 and c_1 are arbitrary complex numbers satisfying a normalisation condition given in eqn (S2).

$$|c_0|^2 + |c_1|^2 = 1 \quad (\text{S2})$$

The quantum state $|\varphi\rangle$ in eqn (S1) can also be represented by a matrix as follows:

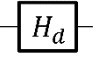


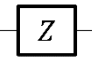
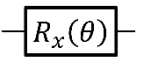
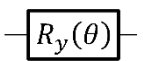
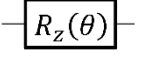
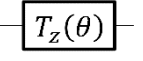
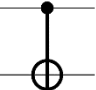
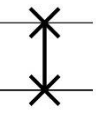
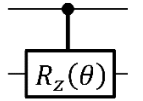
$$|\varphi\rangle = \begin{pmatrix} c_0 \\ c_1 \end{pmatrix} \quad (\text{S3})$$

Quantum gates acting on one qubit can be expressed by a (2×2) unitary matrix and the quantum state after the quantum gate application can be calculated by matrix algebra. For example, the quantum state after the application of an Hadamard gate can be calculated as in eqn (S4).

$$H_d|\varphi\rangle = \frac{1}{\sqrt{2}} \begin{pmatrix} 1 & 1 \\ 1 & -1 \end{pmatrix} \begin{pmatrix} c_0 \\ c_1 \end{pmatrix} = \frac{1}{\sqrt{2}} \begin{pmatrix} c_0 + c_1 \\ c_0 - c_1 \end{pmatrix} \quad (\text{S4})$$

The circuit symbols and matrix representations of the quantum gates used for quantum chemical calculations are summarised in Table S1. In the quantum circuit, the horizontal lines specify a qubit or N -qubits, and squares, circles, and vertical lines represent quantum gates, which are applied to qubits from left to right order.

Table S1. Graph and matrix representations of quantum gates.

Gate	Circuit symbol	Matrix representation
Hadamard (H_d)		$\frac{1}{\sqrt{2}} \begin{pmatrix} 1 & 1 \\ 1 & -1 \end{pmatrix}$
Pauli-X		$\begin{pmatrix} 0 & 1 \\ 1 & 0 \end{pmatrix}$
Pauli-Y		$\begin{pmatrix} 0 & -i \\ i & 0 \end{pmatrix}$
Pauli-Z		$\begin{pmatrix} 1 & 0 \\ 0 & -1 \end{pmatrix}$
$R_x(\theta)$		$\begin{pmatrix} \cos \frac{\theta}{2} & -i \sin \frac{\theta}{2} \\ -i \sin \frac{\theta}{2} & \cos \frac{\theta}{2} \end{pmatrix}$
$R_y(\theta)$		$\begin{pmatrix} \cos \frac{\theta}{2} & -\sin \frac{\theta}{2} \\ \sin \frac{\theta}{2} & \cos \frac{\theta}{2} \end{pmatrix}$
$R_z(\theta)$		$\begin{pmatrix} e^{-i\theta/2} & 0 \\ 0 & e^{i\theta/2} \end{pmatrix}$
$T_z(\theta)$		$\begin{pmatrix} 1 & 0 \\ 0 & e^{i\theta} \end{pmatrix}$
Controlled-NOT (CNOT)		$\begin{pmatrix} 1 & 0 & 0 & 0 \\ 0 & 1 & 0 & 0 \\ 0 & 0 & 0 & 1 \\ 0 & 0 & 1 & 0 \end{pmatrix}$
SWAP		$\begin{pmatrix} 1 & 0 & 0 & 0 \\ 0 & 0 & 1 & 0 \\ 0 & 1 & 0 & 0 \\ 0 & 0 & 0 & 1 \end{pmatrix}$
Controlled- $R_z(\theta)$		$\begin{pmatrix} 1 & 0 & 0 & 0 \\ 0 & 1 & 0 & 0 \\ 0 & 0 & e^{-i\theta/2} & 0 \\ 0 & 0 & 0 & e^{i\theta/2} \end{pmatrix}$

2. Computational conditions for quantum chemical calculations

In this study, we performed quantum chemical calculations of vertical ionisation energies, singlet–triplet energy gaps, and vertical excitation energies of light atoms and small molecules. We used experimentally reported equilibrium geometries except for NCN, CNN, dihalocarbenes (CX_2), dihalosilylenes (SiX_2), and formaldehyde (HCHO). For NCN and CNN, we carried out geometry optimisations at the UB3LYP/6-311G(d,p) level. For dihalocarbenes, dihalosilylenes, and formaldehyde we used the B3LYP/6-31G(d) method to optimise the ground state geometry. Geometry optimisations were performed by using Gaussian 09 (Revision B.01) software.^[S1] Cartesian coordinates of molecules under study are listed below.

In the vertical ionisation energy calculations, we adopted the active space approximation and executed the CAS-CI/6-311G(d,p) calculations for both neutral and ionised states. We used the same active space as in the previous study by using the BxB quantum algorithm,^[S2] namely (1s, 2s) for He atom, (1s, 2s, 2p) for other atoms, and active space given in Supporting Information of Ref. S2 for HF, BF, CF, CO, O₂, NO, CN, F₂, H₂O, and NH₃. Active spaces of CH₄, HCN, and HNC molecules are given in Fig. S1–S3, respectively. All the CAS-CI calculations for both their neutral and cationic states were carried out by using the RHF/ROHF canonical orbitals of the neutral states.

In the singlet–triplet energy gap calculations, the active spaces for C and O atoms are (1s, 2s, 2p), and those for NH, OH⁺, NF, NCN, and CNN molecules are depicted in Fig. S4–S8, respectively. The singlet–triplet energy gap calculations at the CAS-CI method were executed by using the ROHF/6-311G(d,p) wave function for the spin-triplet state as the reference.

Active spaces for the vertical excitation energies of dihalocarbenes and dihalosilylenes consist of four lone pairs of halogen atoms in addition to HOMO and LUMO, and the resultant active space is (10e, 6o) as illustrated in Fig. S9–S13. We used the RHF/6-31G* wave functions as the reference.

All single point calculations were carried out by using GAMESS-US program.^[S3]

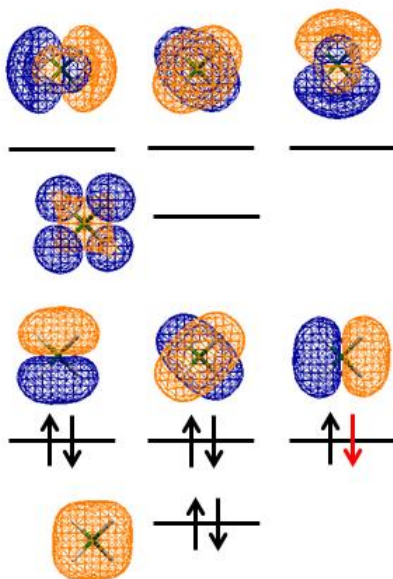


Fig. S1 The CAS-CI active space of CH₄ molecule. Arrows specify the Hartree–Fock electronic configuration in the neutral ground state. A red arrow is the electron to be ionised.

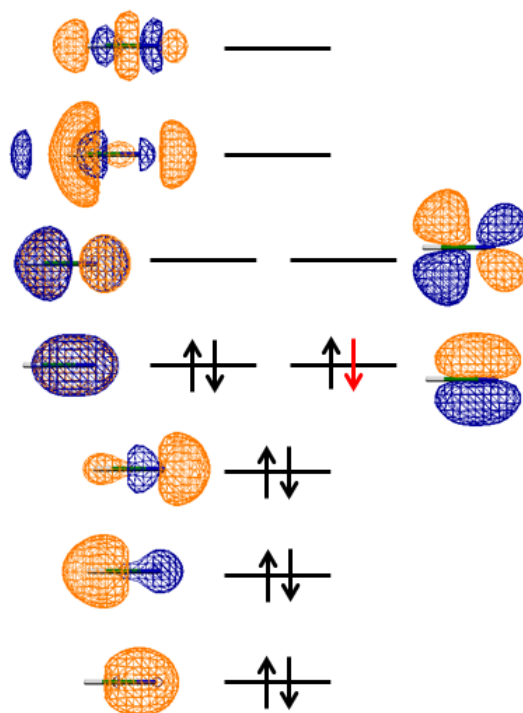


Fig. S2 The CAS-CI active space of HCN molecule. Arrows specify the Hartree–Fock electronic configuration in the neutral ground state. A red arrow is the electron to be ionised.

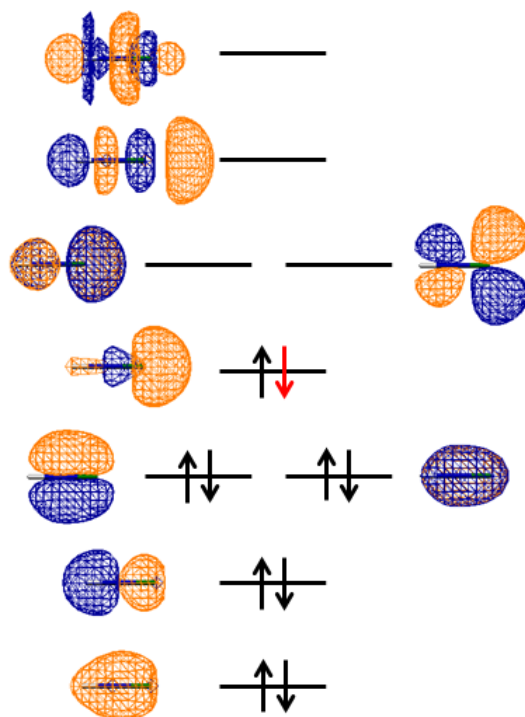


Fig. S3 The CAS-CI active space of HNC molecule. Arrows specify the Hartree–Fock electronic configuration in the neutral ground state. A red arrow is the electron to be ionised.

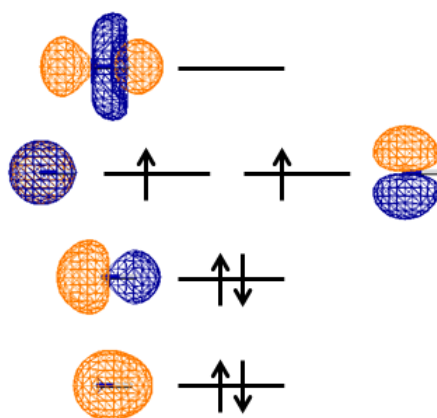


Fig. S4 The CAS-CI active space of NH molecule. Arrows specify the Hartree–Fock electronic configuration in the lowest spin-triplet state.

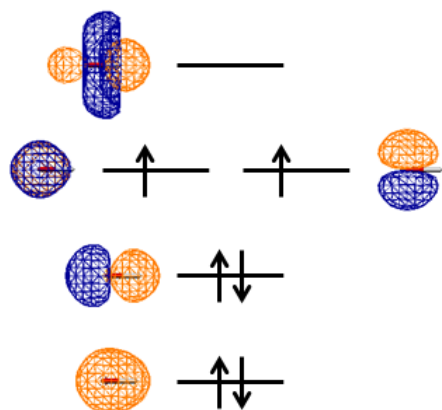


Fig. S5 The CAS-CI active space of OH⁺ molecule. Arrows specify the Hartree-Fock electronic configuration in the lowest spin-triplet state.

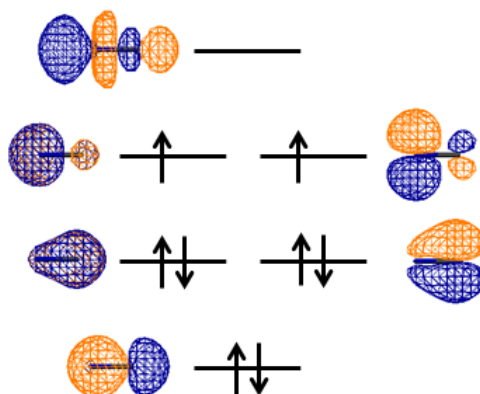


Fig. S6 The CAS-CI active space of NF molecule. Arrows specify the Hartree-Fock electronic configuration in the lowest spin-triplet state.

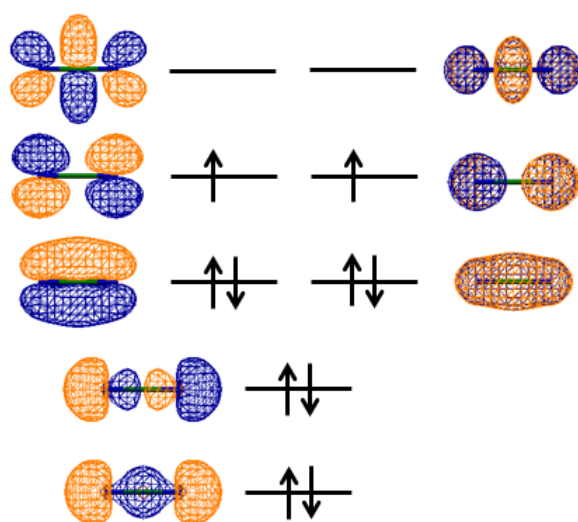


Fig. S7 The CAS-CI active space of NCN molecule. Arrows specify the Hartree-Fock electronic configuration in the lowest spin-triplet state.

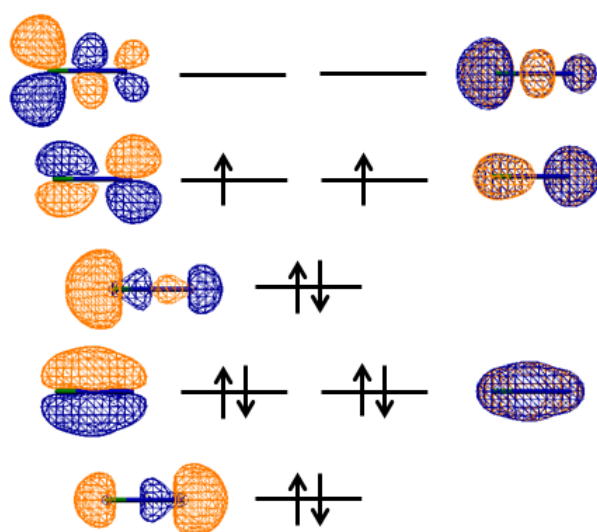


Fig. S8 The CAS-CI active space of CNN molecule. Arrows specify the Hartree–Fock electronic configuration in the lowest spin-triplet state.

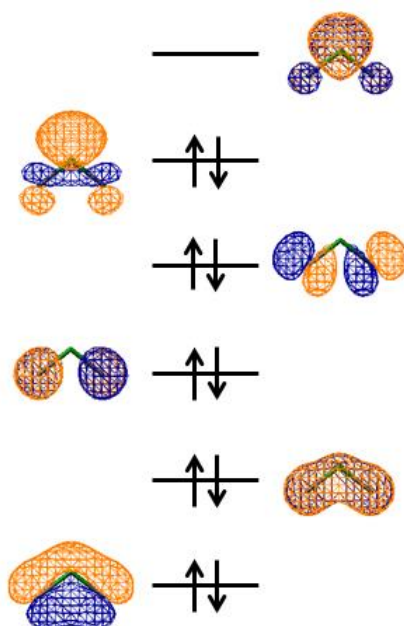


Fig. S9 The CAS-CI active space of CF₂ molecule. Arrows specify the Hartree–Fock electronic configuration in the electronic ground state.

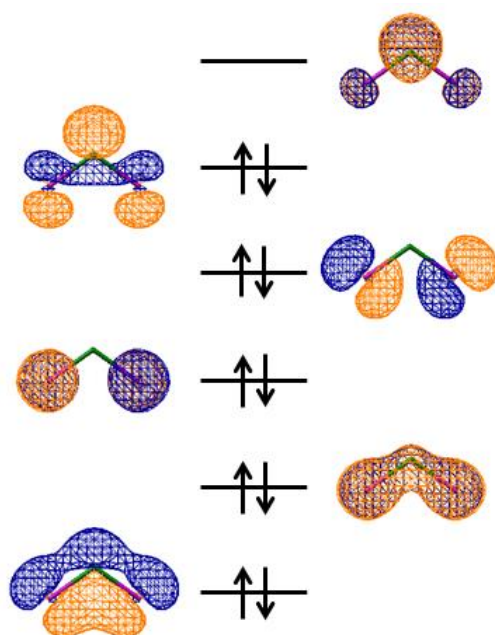


Fig. S10 The CAS-CI active space of CCl_2 molecule. Arrows specify the Hartree-Fock electronic configuration in the electronic ground state.

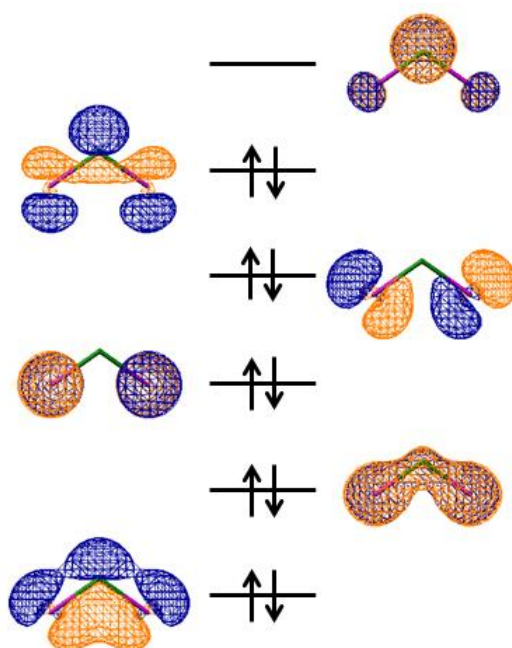


Fig. S11 The CAS-CI active space of CBr_2 molecule. Arrows specify the Hartree-Fock electronic configuration in the electronic ground state.

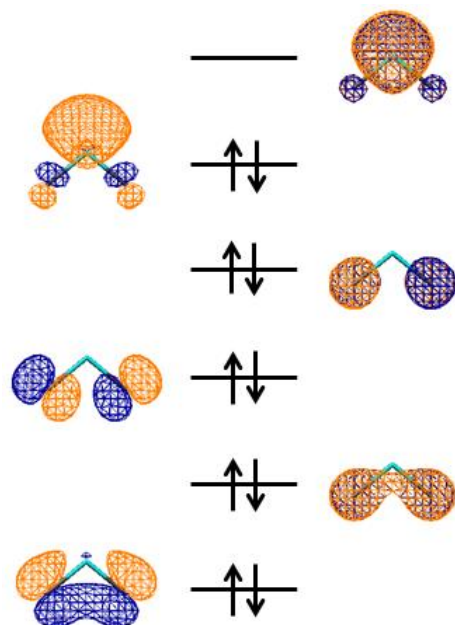


Fig. S12 The CAS-CI active space of SiF_2 molecule. Arrows specify the Hartree–Fock electronic configuration in the electronic ground state.

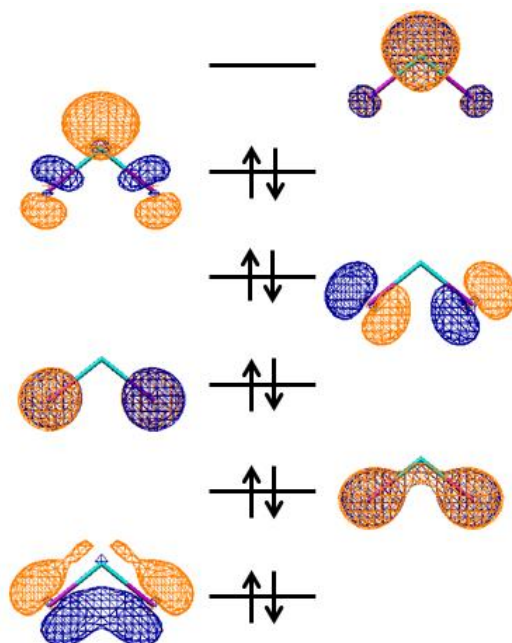


Fig. S13 The CAS-CI active space of SiCl_2 molecule. Arrows specify the Hartree–Fock electronic configuration in the electronic ground state.

Cartesian coordinates of HF molecule
H 0.000000 0.000000 0.000000
F 0.000000 0.000000 0.916800

Cartesian coordinates of BF molecule
B 0.000000 0.000000 0.000000
F 0.000000 0.000000 1.262670

Cartesian coordinates of CF molecule
C 0.000000 0.000000 0.000000
F 0.000000 0.000000 1.276000

Cartesian coordinates of CO molecule
C 0.000000 0.000000 0.000000
O 0.000000 0.000000 1.128200

Cartesian coordinates of O₂ molecule
O 0.000000 0.000000 0.000000
O 0.000000 0.000000 1.208000

Cartesian coordinates of NO molecule
N 0.000000 0.000000 0.000000
O 0.000000 0.000000 1.150800

Cartesian coordinates of CN molecule
C 0.000000 0.000000 0.000000
N 0.000000 0.000000 1.171800

Cartesian coordinates of F₂ molecule
F 0.000000 0.000000 0.000000
F 0.000000 0.000000 1.411900

Cartesian coordinates of H₂O molecule
O 0.000000 0.000000 0.117416
H 0.000000 0.757541 -0.469664
H 0.000000 -0.757541 -0.469664

Cartesian coordinates of NH₃ molecule

N	0.000000	0.114487	0.000000
H	-0.937703	-0.267137	0.000000
H	0.468851	-0.267137	0.812075
H	0.468851	-0.267137	-0.812075

Cartesian coordinates of CH₄ molecule

C	0.000000	0.000000	0.000000
H	0.627600	0.627600	0.627600
H	-0.627600	-0.627600	0.627600
H	-0.627600	0.627600	-0.627600
H	0.627600	-0.627600	-0.627600

Cartesian coordinates of HCN molecule

H	0.000000	0.000000	-1.064000
C	0.000000	0.000000	0.000000
N	0.000000	0.000000	1.156000

Cartesian coordinates of HNC molecule

H	0.000000	0.000000	-0.986000
N	0.000000	0.000000	0.000000
C	0.000000	0.000000	1.173000

Cartesian coordinates of NH molecule

N	0.000000	0.000000	0.000000
H	0.000000	0.000000	1.036200

Cartesian coordinates of OH⁺ molecule

O	0.000000	0.000000	0.000000
H	0.000000	0.000000	1.036200

Cartesian coordinates of NF molecule

N	0.000000	0.000000	0.000000
F	0.000000	0.000000	1.317000

Cartesian coordinates of NCN molecule

N	0.000000	0.000000	1.226249
C	0.000000	0.000000	0.000000
N	0.000000	0.000000	-1.226249

Cartesian coordinates of CNN molecule

C	0.000000	0.000000	-1.286441
N	0.000000	0.000000	-0.050924
N	0.000000	0.000000	1.153587

Cartesian coordinates of CF₂ molecule

F	0.000000	1.035667	-0.201987
C	0.000000	0.000000	0.605962
F	0.000000	-1.035667	-0.201987

Cartesian coordinates of CCl₂ molecule

Cl	0.000000	1.429977	-0.152156
C	0.000000	0.000000	0.862218
Cl	0.000000	-1.429977	-0.152156

Cartesian coordinates of CBr₂ molecule

Br	0.000000	1.565800	-0.087405
C	0.000000	0.000000	1.019729
Br	0.000000	-1.565800	-0.087405

Cartesian coordinates of SiF₂ molecule

F	0.000000	1.246082	-0.450129
Si	0.000000	0.000000	0.578738
F	0.000000	-1.246082	-0.450129

Cartesian coordinates of SiCl₂ molecule

Cl	0.000000	1.642083	-0.386162
Si	0.000000	0.000000	0.937823
Cl	0.000000	-1.642083	-0.386162

Cartesian coordinates of HCHO molecule

O	0.000000	0.000000	0.677534
C	0.000000	0.000000	-0.528862
H	0.000000	0.937777	-1.123552
H	0.000000	-0.937777	-1.123552

3. Quantum circuits for the state preparations and controlled-*Excit* operations

In the BPDE algorithm, generation of the quantum state in the superposition of ground and excited states by applying a controlled-*Excit* gate is the key step. In this work, we used the Jordan–Wigner transformation for fermion–qubit mapping, and therefore each qubit stores an occupation number of a particular spin orbital ($|1\rangle$ if the spin orbital is occupied by an electron, otherwise $|0\rangle$). In this representation, the Hartree–Fock wave function can be generated by applying Pauli-X gates to N_{elec} of qubits corresponding occupied orbitals, where N_{elec} denotes the number of electrons.

The quantum circuits for the controlled-*Excit* operations in the calculations of vertical ionisation energies, singlet–triplet energy gaps, and vertical excitation energies are illustrated in Fig. S14–S16, respectively, in conjunction with the quantum circuits for the preparation of $|\Psi_0\rangle = |\Psi_{\text{HF}}\rangle$ or $|\Psi_{\text{CSF}}\rangle$.

In the calculations of vertical ionisation energies, $|\Psi_0\rangle$ is the Hartree–Fock wave function of the neutral state. The controlled-*Excit* gate becomes a CNOT gate with the ancillary qubit as the control and the qubit storing the electron occupancy of the spin orbital of which electron ionisation occurs as the target, as illustrated in blue in Fig. S14.

The quantum circuit for the wave function preparation and controlled-*Excit* gate in the direct calculation of singlet–triplet energy gaps are slightly longer than that in the vertical ionisation energy calculations, because we used the configuration state function of the $M_S = 0$ of spin-triplet state as $|\Psi_0\rangle$. The CSF of the spin-triplet state is given in eqn (26) in the main text, and it consists of two Slater determinants. The CSF can be generated by generating one of the Slater determinants in CSF ($|2\alpha\beta\rangle$ for Fig. S15), and another Slater determinant is prepared by applying an Hadamard gate and following three CNOT gates, as illustrated in Fig. S15. The CSF of the spin-singlet state given in eqn (27) in the main text is in the negative linear combination of the two Slater determinants, and thus controlled-*Excit* operation can be accomplished by a controlled-Z operation.

In the vertical excitation energy calculations, the quantum circuit in Fig. S16 is used. In this quantum circuit, the controlled-*Excit* operation corresponds to the symmetry-adapted excitation operations as defined in eqn (28) and (29) in the main text. The quantum circuit for the controlled-*Excit* operation consists of controlled-Hadamard and following four CNOT gates, and one Pauli-Z gate. The last Pauli-Z gate in the parenthesis in Fig. S16 is required for the calculation of singlet–singlet excitation energies. For the calculations of singlet–triplet spin forbidden excitation energies, the Pauli-Z gate should be removed.

The quantum gates corresponding to the controlled-*Excit*[†] gate can be achieved by applying the controlled-*Excit* gate depicted in Fig. S14–S16 in the reversed order (Pauli-Z, and following four CNOT gates and controlled-Hadamard gate in the calculations of vertical excitation energies).

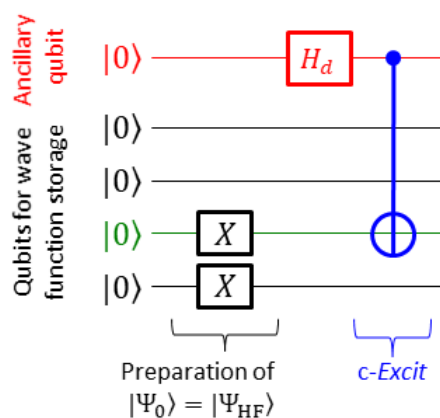


Fig. S14 An example of the quantum circuit for the wave function preparation and controlled-*Excit* operation in the direct calculation of vertical ionisation energies using the BPDE algorithm. The qubit written in red is the ancillary qubit and that in green is the qubit storing the electron occupancy of the spin orbital of which electron ionisation occurs.

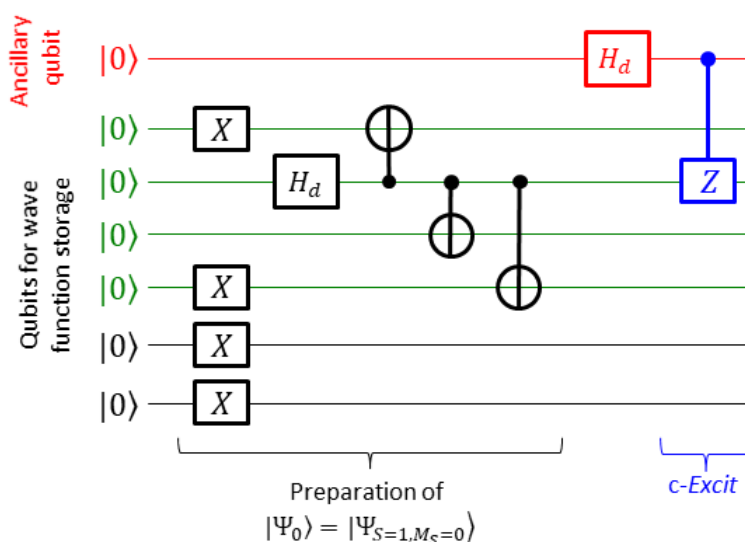


Fig. S15 An example of the quantum circuit for the wave function preparation and controlled-*Excit* operation in the direct calculation of singlet–triplet energy gaps using the BPDE algorithm. The qubit written in red is the ancillary qubit. Qubits in green store the occupation number of singly occupied molecular orbitals (SOMOs) and those in black possess the occupation number of doubly occupied orbitals.

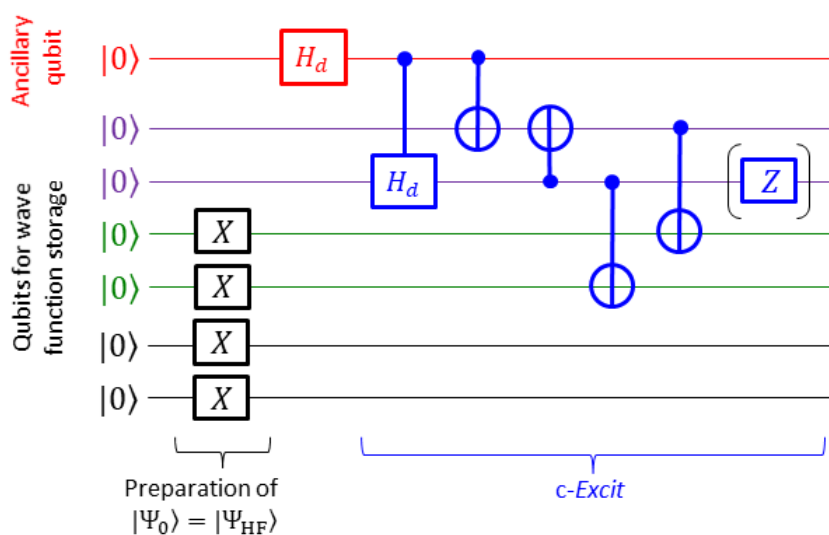


Fig. S16 An example of the quantum circuit for the wave function preparation and controlled-*Excit* operation in the direct calculation of vertical excitation energies using the BPDE algorithm. The qubit written in red is the ancillary qubit. Electron excitation occurs from the qubits in green to the qubits in purple. The Pauli-Z gate in the parenthesis is required for the calculations of singlet–singlet spin allowed electron excitations, and it should be removed for the calculations of singlet–triplet spin forbidden transitions.

4. Computational conditions for the numerical simulations of the BPDE algorithm

The Bayesian phase difference estimation (BPDE) algorithm for the direct calculation of energy gaps consists of the following steps. (1) Define a prior distribution. (2) Set the time evolution length t from a variance σ^2 of the prior distribution. (3) Draw m samples in the range of $\mu - \sigma^2$ to $\mu + \sigma^2$ with a constant interval, and execute the quantum circuit R times with given t and j to calculate a likelihood function $P(0|j; t)$. Here, μ is the mean of the prior distribution. (4) Fitting the obtained likelihood function by a Gaussian function and calculate a posterior distribution $P(j|0; t)$. (5) If the variance of the posterior distribution is smaller than the threshold, the algorithm returns the mean of the posterior distribution as the estimate of the j value. Otherwise returns to step (2) with the posterior distribution as the prior distribution of the next iteration.

In the step (1), we used a Gaussian function as the prior distribution. In the vertical ionisation energy calculations, we used a mean $\mu = \text{IE}(\Delta\text{SCF}) = E_{\text{HF}}(\text{Cation}) - E_{\text{HF}}(\text{Neutral})$. For singlet–triplet energy gaps we set $\mu = 0$ Hartree. In the vertical excitation energy calculations, the initial estimate is computed from the orbital energy differences, $\mu(j \rightarrow a) = \varepsilon(a) - \varepsilon(j)$. Here we assume that the electronic excited state wave function is mainly described as the electron transition from the j -th occupied to the a -th unoccupied orbitals. The variance of the Gaussian function is set to be $\sigma^2 = 1.0$ Hartree for all calculations.

In the second step, the length of the time evolution of the wave function is set as in eqn (S5). This condition is derived so as to the likelihood function $P(0|j; t)$ has a sufficiently large gradient and $P(0|j; t)$ has a single maximum in the range of $\mu - \sigma^2 \leq j \leq \mu + \sigma^2$.

$$t = 1.8/\sigma^2 \quad (\text{S5}).$$

In the step (3), we used $m = 21$ and $R = 1,000$. The threshold used for convergence check in the step (5) was set to 0.005 Hartree, unless otherwise stated.

The quantum circuit for the BPDE algorithm contains the time evolution operator $U = \exp(-iHt)$. In this work, the molecular Hamiltonian H is transformed to the qubit Hamiltonian consisting of a linear combination of Pauli strings as in eqn (S6) and (S7), by using Jordan–Wigner transformation (JWT).

$$H = \sum_m^M w_m P_m \quad (\text{S6})$$

$$P_m = \sigma_{N_{\text{SO}}} \otimes \sigma_{N_{\text{SO}}-1} \otimes \cdots \otimes \sigma_1, \quad \sigma_k \in \{I, X, Y, Z\} \quad (\text{S7})$$

The quantum circuit corresponding to the time evolution operator U is constructed by adopting the second-order Trotter decomposition given in eqn (S8). It is known that the Trotter decomposition error depends on the order of Pauli strings in eqn (S8).^[S4,S5] In this work, we used the magnitude ordering, in which Pauli strings are ordered by the absolute value of the norm of Pauli strings $|w_m|$.

$$U \approx \left[\prod_{m=1}^M \exp(-iw_m P_m t/2N) \times \prod_{m=M}^1 \exp(-iw_m P_m t/2N) \right]^N \quad (\text{S8})$$

5. Computational conditions for the numerical simulations of the BPE algorithm

In this work, we also calculated the energy gaps using a naïve approach based on two separate BPE simulations. The computational steps of BPE are very similar to those of BPDE; (1) define a Gaussian function with a mean μ and a variance σ^2 as the prior distribution, (2) draw m samples in the range of $\mu - \sigma^2$ to $\mu + \sigma^2$ with a constant interval, and execute the quantum circuit R times, (3) fitting the obtained the likelihood function by a Gaussian function, (4) compute the posterior distribution, (5) if the variance of the posterior distribution is smaller than the threshold, return the mean of the posterior distribution as the estimate of the eigenenergy, otherwise returns to step (2) with the posterior distribution as the prior distribution of the next step.

In this study, we used the energy expectation value of the reference wave function as the initial estimate of the total energy. The reference wave function is set as the single determinant wave function with the RHF or ROHF electronic configurations for closed shell singlet and triplet states, respectively. For the open shell singlet states in the calculation of singlet–triplet energy gaps and the spin-singlet excited states, we used a configuration state function (CSF) defined in eqn (S9) as the reference wave function.

$$|\Psi_{\text{CSF}}\rangle = \frac{1}{\sqrt{2}}(|2 \cdots 2\alpha\beta 0 \cdots 0\rangle - |2 \cdots 2\beta\alpha 0 \cdots 0\rangle) \quad (\text{S9})$$

Here, 2, α , β , and 0 specify the doubly occupied orbitals, singly occupied orbitals with a spin- α electron, singly occupied orbitals with a spin- β electron, and unoccupied orbitals, respectively.

Variance of the prior distribution is defined by using the energy expectation value of the reference wave function E_{Ref} , as in eqn (S10).

$$\sigma^2 = \max[|0.05 \times E_{\text{Ref}}|, 1.0] \quad (\text{S10})$$

For other simulation conditions including the number of samples m and the repetition number of the quantum circuit R , evolution time length at each Bayesian step, and convergence threshold, we use the same values as the BPDE quantum circuit simulations.

6. List of the calculated energies and energy gaps

In quantum computers, whether the measurement yields either 0 or 1 is probabilistic, and therefore energies and energy gaps computed by using the BPE and BPDE algorithms vary by each numerical simulation. In this study, we executed five numerical simulations for each molecule/geometry. The vertical ionisation energies computed by BPDE and BPE with the CAS-CI values and experimental ionisation energies are listed in Table S2. The total energy of neutral and cationic states computed by using BPE are summarised in Table S3. The list of the singlet–triplet energy gaps and the total energies of the spin-singlet and triplet states are given as Tables S4–S7, respectively. The computed vertical ionisation energies, and total energies of the electronic ground and excited states are summarised in Tables S8 and S9, respectively.

Table S2. Vertical ionisation energies computed by using BPE, BPDE, and CAS-CI methods.

System	IE(BPE)/eV	IE(BPDE)/eV	IE(CAS-CI)/eV	IE(Exptl.)/eV
He	23.9100	23.9114	23.8989	24.58741 ^[S6]
	23.9095	23.9120		
	23.9089	23.9085		
	23.9079	23.9093		
	23.9093	23.9105		
Li	5.3432	5.3408	5.3400	5.39172 ^[S6]
	5.3408	5.3431		
	5.3413	5.3409		
	5.3388	5.3419		
	5.3392	5.3409		
Be	8.9285	8.9290	8.9241	9.32263 ^[S6]
	8.9283	8.9271		
	8.9274	8.9287		
	8.9271	8.9277		
	8.9288	8.9284		
B	8.1145	8.1040	8.0984	8.29803 ± 0.00002 ^[S6]
	8.1123	8.1045		
	8.1113	8.1038		
	8.1131	8.1052		
	8.1123	8.1051		
C	11.3661	11.3673	11.3424	11.26030 ^[S6]
	11.3703	11.3673		
	11.3665	11.3670		
	11.3685	11.3683		
	11.3712	11.3687		
N	14.9087	14.9128	14.9004	14.53414 ^[S6]
	14.9089	14.9110		
	14.9126	14.9110		
	14.9107	14.9119		
	14.9102	14.9132		
HF	16.8327	16.8292	16.9224	16.03 ± 0.04 ^[S7]
	16.8306	16.8321		
	16.8310	16.8312		
	16.8343	16.8316		
	16.8314	16.8310		

Table S2. (continued)

System	IE(BPE)/eV	IE(BPDE)/eV	IE(CAS-CI)/eV	IE(Exptl.)/eV
BF	11.2817	11.2857	11.2513	11.12 ± 0.01 ^[S7]
	11.2825	11.2835		
	11.2835	11.2846		
	11.2808	11.2832		
	11.2827	11.2853		
CF	9.8286	9.8246	9.8251	9.11 ± 0.01 ^[S7]
	9.8320	9.8259		
	9.8318	9.8252		
	9.8296	9.8264		
	9.8313	9.8246		
CO	14.8019	14.7937	14.8189	14.014 ± 0.0003 ^[S7]
	14.8013	14.7949		
	14.7969	14.7957		
	14.8013	14.7950		
	14.8013	14.7976		
O ₂	12.7166	12.7227	12.7018	12.0697 ± 0.0002 ^[S7]
	12.7058	12.7250		
	12.7167	12.7222		
	12.7130	12.7244		
	12.7101	12.7226		
NO	9.9061	9.9100	9.8793	9.2642 ± 0.00002 ^[S7]
	9.9087	9.9100		
	9.9083	9.9106		
	9.9036	9.9068		
	9.9037	9.9099		
CN	14.3783	14.3634	14.3792	13.598 ^[S7]
	14.3693	14.3651		
	14.3692	14.3644		
	14.3670	14.3637		
	14.3599	14.3637		
F ₂	16.5108	16.5030	16.5006	15.697 ± 0.003 ^[S7]
	16.4989	16.5007		
	16.4895	16.5059		
	16.4926	16.5033		
	16.5053	16.5033		

Table S2. (continued)

System	IE(BPE)/eV	IE(BPDE)/eV	IE(CAS-CI)/eV	IE(Exptl.)/eV
H ₂ O	13.3091	13.3127	13.2722	12.621 ± 0.002 ^[S7]
	13.3118	13.3105		
	13.3108	13.3124		
	13.3096	13.3125		
	13.3100	13.3116		
NH ₃	11.3629	11.3606	11.3510	10.070 ± 0.020 ^[S7]
	11.3634	11.3626		
	11.3615	11.3607		
	11.3629	11.3651		
	11.3613	11.3624		
CH ₄	14.4881	14.4896	14.4980	12.61 ± 0.01 ^[S7]
	14.4896	14.4898		
	14.4870	14.4884		
	14.4863	14.4888		
	14.4865	14.4899		
HCN	13.7484	13.7419	13.7326	13.60 ± 0.01 ^[S7]
	13.7365	13.7424		
	13.7498	13.7400		
	13.7441	13.7442		
	13.7475	13.7424		
HNC	12.2635	12.2579	12.2697	12.5 ± 0.1 ^[S7]
	12.2621	12.2566		
	12.2600	12.2576		
	12.2590	12.2567		
	12.2624	12.2572		

Table S3. Total energies of neutral and cationic states calculated by using BPE and CAS-CI methods.

System	E(Neutral)/Hartree		E(Cationic)/Hartree	
	BPE	CAS-CI	BPE	CAS-CI
He	-2.8659959021	-2.8680014755	-1.9873215197	-1.9897314528
	-2.8660438243			
	-2.8660198845			
	-2.8659737863			
	-2.8660304575			
Li	-7.4321510873	-7.4321126921	-7.2357906619	-7.2358722241
	-7.4320929774			
	-7.4320807473			
	-7.4320550112			
	-7.4321484486			
Be	-14.5909912913	-14.5909577588	-14.2628747036	-14.2630020916
	-14.5911005783			
	-14.5910464010			
	-14.5910535229			
	-14.5910541500			
B	-24.5465988239	-24.5465615624	-24.2483965921	-24.2489516259
	-24.5465223807			
	-24.5464879314			
	-24.5465636811			
	-24.5465119259			
C	-37.6968597343	-37.6972661038	-37.2791638430	-37.2804416397
	-37.6968914401			
	-37.6969719757			
	-37.6969132525			
	-37.6969739051			
N	-54.3947793638	-54.3947771214	-53.8468957268	-53.8471993560
	-54.3947482917			
	-54.3947750481			
	-54.3947877732			
	-54.3947274013			

Table S3. (continued)

System	E(Neutral)/Hartree		E(Cationic)/Hartree	
	BPE	CAS-CI	BPE	CAS-CI
HF	-100.0434914758	-100.0521327804	-99.4249006029	-99.4302478078
	-100.0434704099		-99.4249579541	
	-100.0434731555		-99.4249450396	
	-100.0435424290		-99.4248918361	
	-100.0434366460		-99.4248933914	
BF	-124.1556887841	-124.1566657988	-123.7410927837	-123.7431873460
	-124.1555977135		-123.7409729305	
	-124.1556282345		-123.7409672202	
	-124.1556594673		-123.7410983577	
	-124.1556671175		-123.7410346514	
CF	-137.2179020514	-137.2178006798	-136.8567096685	-136.8567363909
	-137.2178673541		-136.8565494768	
	-137.2179200122		-136.8566099964	
	-137.2177459608		-136.8565161398	
	-137.2178773520		-136.8565844018	
CO	-112.8205039749	-112.8221087096	-112.2765445289	-112.2775225244
	-112.8204446701		-112.2765073229	
	-112.8203461029		-112.2765707739	
	-112.8204723396		-112.2765341565	
	-112.8204487741		-112.2765128261	
O ₂	-149.6967983826	-149.6980911449	-149.2294723576	-149.2313098822
	-149.6969995313		-149.2300691449	
	-149.6970258825		-149.2296962610	
	-149.6969758029		-149.2297831196	
	-149.6969539234		-149.2298680032	
NO	-129.3276858961	-129.3289813017	-128.9636438053	-128.9659259785
	-129.3277236954		-128.9635853342	
	-129.3277792130		-128.9636554763	
	-129.3276324716		-128.9636804348	
	-129.3276971921		-128.9637413759	

Table S3. (continued)

System	E(Neutral)/Hartree		E(Cationic)/Hartree	
	BPE	CAS-CI	BPE	CAS-CI
CN	-92.2721732833	-92.2729303806	-91.7437811392	-91.7445032326
	-92.2717351417		-91.7436732882	
	-92.2719375879		-91.7438806550	
	-92.2719053928		-91.7439294873	
	-92.2716185210		-91.7439025433	
F ₂	-198.7859716043	-198.7870071634	-198.1796975910	-198.1806201316
	-198.7858749400		-198.1796649683	
	-198.7859262165		-198.1797720727	
	-198.7859374244		-198.1796316945	
	-198.7859480699		-198.1796746898	
H ₂ O	-76.0577278965	-76.0570903787	-75.5686285862	-75.5693451898
	-76.0577903695		-75.5685918569	
	-76.0577607396		-75.5685997850	
	-76.0577595473		-75.5686418127	
	-76.0577560444		-75.5686217840	
NH ₃	-56.2244597378	-56.2255975414	-55.8068817148	-55.8084543738
	-56.2244839679		-55.8068879376	
	-56.2244117048		-55.8068829061	
	-56.2244853092		-55.8069059412	
	-56.2244230678		-55.8069042788	
CH ₄	-40.2344539278	-40.2375738474	-39.7020259354	-39.7047841484
	-40.2344028347		-39.7019215243	
	-40.2344457846		-39.7020601333	
	-40.2344043330		-39.7020442973	
	-40.2343213985		-39.7019521904	
HCN	-92.9691523223	-92.9717131658	-92.4639085061	-92.4670495354
	-92.9687840862		-92.4639758721	
	-92.9690984240		-92.4638019111	
	-92.9690663393		-92.4639791111	
	-92.9691100087		-92.4638989304	

Table S3. (continued)

System	E(Neutral)/Hartree		E(Cationic)/Hartree	
	BPE	CAS-CI	BPE	CAS-CI
HNC	-92.9419116022	-92.9435577522	-92.4912370882	-92.4926553564
	-92.9418195978		-92.4911964745	
	-92.9418225176		-92.4912746029	
	-92.9417910864		-92.4912800361	
	-92.9417841977		-92.4911498349	

Table S4. Singlet–triplet energy gaps of H₂ molecule computed by using BPE, BPDE, and full-CI methods.

R(H⋯H)/Å	$\Delta E_{S-T}/\text{kcal mol}^{-1}$		
	BPE	BPDE	Full-CI
1.2	-141.3421	-141.3464	-143.2589
	-141.3584	-141.3065	
	-141.3570	-141.3177	
	-141.2650	-141.3580	
	-141.3498	-141.3469	
1.3	-112.9621	-112.9608	-112.9205
	-112.9539	-112.9596	
	-112.9091	-112.9165	
	-112.9140	-112.9708	
	-112.9172	-112.9476	
1.4	-87.1034	-86.8616	-87.8766
	-86.7693	-86.8602	
	-87.1294	-86.8956	
	-86.9485	-86.9544	
	-86.8611	-86.9773	
1.5	-66.6526	-66.7835	-67.4980
	-66.7828	-66.6975	
	-66.7397	-66.7056	
	-66.7156	-66.6199	
	-66.6419	-66.6774	
1.6	-51.4313	-51.3994	-51.1805
	-51.4049	-51.4091	
	-51.4113	-51.3584	
	-51.3638	-51.3415	
	-51.3315	-51.3618	
1.7	-38.3218	-38.3331	-38.3343
	-38.3789	-38.3590	
	-38.4030	-38.3711	
	-38.3814	-38.3893	
	-38.3999	-38.4074	

Table S4. (continued)

R(H \cdots H)/Å	$\Delta E_{S-T}/\text{kcal mol}^{-1}$		
	BPE	BPDE	Full-CI
1.8	-28.4756	-28.4782	-28.3897
	-28.4455	-28.4269	
	-28.4542	-28.4304	
	-28.4700	-28.4949	
	-28.4819	-28.4693	
1.9	-20.5479	-20.4861	-20.8143
	-20.5248	-20.5473	
	-20.4996	-20.4684	
	-20.4639	-20.4968	
	-20.5228	-20.4787	
2.0	-15.0985	-15.0878	-15.1252
	-15.0270	-15.0596	
	-15.0593	-15.0925	
	-15.1169	-15.0632	
	-15.0789	-15.0550	
2.1	-10.9627	-10.9296	-10.9075
	-10.8966	-10.9517	
	-10.9793	-10.9542	
	-10.9085	-10.9167	
	-10.9751	-10.9171	
2.2	-7.8490	-7.8235	-7.8129
	-7.8611	-7.8212	
	-7.8035	-7.8771	
	-7.7862	-7.8122	
	-7.8259	-7.8830	
2.3	-5.5825	-5.5321	-5.5622
	-5.5945	-5.5436	
	-5.5292	-5.5450	
	-5.6165	-5.5562	
	-5.5334	-5.5654	

Table S4. (continued)

R(H···H)/Å	$\Delta E_{S-T}/\text{kcal mol}^{-1}$		
	BPE	BPDE	Full-CI
2.4	-3.8920	-3.9307	-3.9370
	-3.9481	-3.9081	
	-3.8978	-3.9417	
	-3.9157	-3.8975	
	-3.9010	-3.8687	
2.5	-2.7507	-2.7236	-2.7710
	-2.7126	-2.7264	
	-2.7075	-2.7456	
	-2.7514	-2.7128	
	-2.7694	-2.7505	
2.6	-1.8980	-1.8775	-1.9389
	-1.9464	-1.8906	
	-1.9334	-1.9804	
	-1.9139	-1.9408	
	-1.9398	-1.9191	
2.7	-1.3538	-1.3140	-1.3486
	-1.3326	-1.3244	
	-1.3073	-1.3356	
	-1.3302	-1.3511	
	-1.3172	-1.3682	
2.8	-0.9187	-0.9777	-0.9320
	-0.8996	-0.9349	
	-0.9797	-0.9079	
	-0.9202	-0.9318	
	-0.8502	-0.9809	
2.9	-0.6526	-0.6497	-0.6399
	-0.6515	-0.6247	
	-0.6445	-0.6314	
	-0.6328	-0.6207	
	-0.6267	-0.6089	

Table S4. (continued)

R(H···H)/Å	$\Delta E_{S-T}/\text{kcal mol}^{-1}$		
	BPE	BPDE	Full-CI
3.0	-0.4009	-0.4212	-0.4364
	-0.4414	-0.4291	
	-0.4079	-0.4319	
	-0.4055	-0.4634	
	-0.4688	-0.4340	

Table S5. Total energies of the spin-singlet and triplet states of H₂ molecule calculated by using BPE and full-CI methods.

R(H···H)/Å	E(Singlet)/Hartree		E(Triplet)/Hartree	
	BPE	full-CI	BPE	full-CI
1.2	-1.0536789921	-1.0567411093	-0.8284362380	-0.8284436540
	-1.0536736847		-0.8284049515	
	-1.0537400001		-0.8284734968	
	-1.0535158733		-0.8283959920	
	-1.0537269259		-0.8284718436	
1.3	-1.0352253950	-1.0351866132	-0.8552089221	-0.8552365279
	-1.0352920705		-0.8552886597	
	-1.0352201559		-0.8552882102	
	-1.0352220443		-0.8552822351	
	-1.0352223718		-0.8552775896	
1.4	-1.0142381892	-1.0154682881	-0.8754301750	-0.8754281145
	-1.0137215691		-0.8754459584	
	-1.0143151620		-0.8754657732	
	-1.0139472673		-0.8753860856	
	-1.0138620553		-0.8754401343	
1.5	-0.9968036907	-0.9981486686	-0.8905861082	-0.8905838210
	-0.9970279495		-0.8906028898	
	-0.9969385756		-0.8905821368	
	-0.9968658564		-0.8905478771	
	-0.9967986203		-0.8905980062	
1.6	-0.9839078831	-0.9834735443	-0.9019470314	-0.9019123008
	-0.9838174857		-0.9018985887	
	-0.9837941207		-0.9018651242	
	-0.9838127275		-0.9019593743	
	-0.9837680330		-0.9019660743	
1.7	-0.9714698838	-0.9714270717	-0.9104003348	-0.9103375818
	-0.9714635446		-0.9103029031	
	-0.9715430316		-0.9103439906	
	-0.9714923718		-0.9103277250	
	-0.9714842385		-0.9102902084	

Table S5. (continued)

R(H···H)/Å	E(Singlet)/Hartree		E(Triplet)/Hartree	
	BPE	CAS-CI	BPE	CAS-CI
1.8	-0.9619457476	-0.9618165605	-0.9165669641	-0.9165747769
	-0.9619246300		-0.9165938005	
	-0.9619175696		-0.9165728987	
	-0.9619738735		-0.9166040966	
	-0.9619086030		-0.9165197978	
1.9	-0.9538750105	-0.9543390636	-0.9211299213	-0.9211694615
	-0.9538676397		-0.9211593053	
	-0.9538157582		-0.9211475147	
	-0.9538239750		-0.9212126723	
	-0.9538908936		-0.9211857526	
2.0	-0.9485407994	-0.9486406580	-0.9244798480	-0.9245371332
	-0.9484776570		-0.9245305733	
	-0.9485909264		-0.9245924238	
	-0.9485605341		-0.9244701828	
	-0.9485342608		-0.9245045007	
2.1	-0.9444122375	-0.9443753581	-0.9269421241	-0.9269931513
	-0.9443713340		-0.9270064937	
	-0.9444652481		-0.9269686544	
	-0.9443901084		-0.9270063992	
	-0.9445075920		-0.9270177350	
2.2	-0.9412474302	-0.9412245382	-0.9287393157	-0.9287739635
	-0.9412862563		-0.9287587718	
	-0.9412744110		-0.9288387027	
	-0.9412026092		-0.9287945420	
	-0.9412501794		-0.9287787961	
2.3	-0.9389285432	-0.9389228817	-0.9300322964	-0.9300590149
	-0.9389718445		-0.9300564006	
	-0.9388986116		-0.9300872045	
	-0.9389837503		-0.9300333107	
	-0.9389060568		-0.9300880061	

Table S5. (continued)

R(H···H)/Å	E(Singlet)/Hartree		E(Triplet)/Hartree	
	BPE	CAS-CI	BPE	CAS-CI
2.4	-0.9372195539	-0.9372550184	-0.9310172415	-0.9309810321
	-0.9372757152		-0.9309839493	
	-0.9372038705		-0.9309923996	
	-0.9371862687		-0.9309462708	
	-0.9371913019		-0.9309746691	
2.5	-0.9360584264	-0.9360540394	-0.9316748577	-0.9316382503
	-0.9359855355		-0.9316627184	
	-0.9359673361		-0.9316525939	
	-0.9360280694		-0.9316434350	
	-0.9360929573		-0.9316796131	
2.6	-0.9351556244	-0.9351952059	-0.9321310047	-0.9321053378
	-0.9351915758		-0.9320898372	
	-0.9351714939		-0.9320903617	
	-0.9351890734		-0.9321390430	
	-0.9351933210		-0.9321020137	
2.7	-0.9346044538	-0.9345837928	-0.9324470825	-0.9324345994
	-0.9345331785		-0.9324095620	
	-0.9345508002		-0.9324674786	
	-0.9345400407		-0.9324202879	
	-0.9345361783		-0.9324373149	
2.8	-0.9341231312	-0.9341507289	-0.9326591084	-0.9326654279
	-0.9341157320		-0.9326821842	
	-0.9341854660		-0.9326241635	
	-0.9341791288		-0.9327126369	
	-0.9340291510		-0.9326742500	
2.9	-0.9338807592	-0.9338467145	-0.9328407800	-0.9328270071
	-0.9338568325		-0.9328185358	
	-0.9338667547		-0.9328397090	
	-0.9338232381		-0.9328148172	
	-0.9338538691		-0.9328551781	

Table S5. (continued)

R(H···H)/Å	E(Singlet)/Hartree		E(Triplet)/Hartree	
	BPE	CAS-CI	BPE	CAS-CI
3.0	-0.9336429899	-0.9336315594	-0.9330041530	-0.9329361692
	-0.9336462777		-0.9329428303	
	-0.9335832308		-0.9329332768	
	-0.9335906271		-0.9329443677	
	-0.9336691970		-0.9329220442	

Table S6. Singlet–triplet energy gaps computed by using BPE, BPDE, and CAS-CI methods.

System	$\Delta E_{S-T}/\text{kcal mol}^{-1}$			
	BPE	BPDE	CAS-CI	Exptl.
C	36.7596	36.7738	36.8683	29.142 ^[S8]
	36.8309	36.8375		
	36.8673	36.8381		
	36.8781	36.8197		
	36.7642	36.7902		
O	52.2209	52.2323	52.2329	45.369 ^[S8]
	52.1917	52.2067		
	52.2610	52.2574		
	52.2430	52.2051		
	52.2219	52.2184		
NH	45.7423	45.7622	45.7898	35.928 ^[S9]
	45.7400	45.7948		
	45.7241	45.7879		
	45.7412	45.7409		
	45.7333	45.7041		
OH ⁺	56.9526	56.9584	57.0591	50.493 ^[S9]
	56.9847	56.9485		
	56.9818	56.9631		
	56.9544	56.9485		
	57.0086	56.9745		
NF	42.5211	42.6253	42.3015	34.320 ^[S9]
	42.5608	42.6478		
	42.5889	42.6283		
	42.5659	42.6095		
	42.5708	42.6014		
NCN	26.1867	26.1887	26.3132	23.291 ^[S10]
	26.5234	26.1091		
	26.4513	26.2055		
	26.4080	26.1580		
	26.3688	26.1570		

Table S6. (continued)

System	$\Delta E_{S-T}/\text{kcal mol}^{-1}$			
	BPE	BPDE	Full-CI	Exptl.
CNN	23.4295	23.8073	23.6124	19.509 ^[S11]
	23.9067	23.7762		
	23.9710	23.8293		
	23.5825	23.8029		
	23.8707	23.8420		

Table S7. Total energies of the spin-singlet and triplet states of atoms and molecules calculated by using BPE and full-CI methods.

System	E(Singlet)/Hartree		E(Triplet)/Hartree	
	BPE	CAS-CI	BPE	CAS-CI
C	-37.6382387480	-37.6385127952	-37.6968187994	-37.6972661038
	-37.6382151344		-37.6969089026	
	-37.6381864884		-37.6969382816	
	-37.6381593435		-37.6969283595	
	-37.6382737612		-37.6968612409	
O	-74.7170031127	-74.7169792971	-74.8002222739	-74.8002175804
	-74.7170152986		-74.8001880314	
	-74.7169842226		-74.8002673465	
	-74.7169849068		-74.8002392941	
	-74.7170027538		-74.8002235125	
NH	-54.9046676179	-54.9050694497	-54.9775625072	-54.9780401101
	-54.9046249201		-54.9775161794	
	-54.9046663074		-54.9775322332	
	-54.9046071985		-54.9775003825	
	-54.9046111924		-54.9774918425	
OH ⁺	-74.9020728776	-74.9023770882	-74.9928324937	-74.9933065022
	-74.9020764365		-74.9928873167	
	-74.9020418390		-74.9928479764	
	-74.9020748128		-74.9928373865	
	-74.9020337099		-74.9928825536	
NF	-153.7637048601	-153.7598743737	-153.8314665514	-153.8272860423
	-153.7635902514		-153.8314152016	
	-153.7636182154		-153.8314878916	
	-153.7636330907		-153.8314661528	
	-153.7636558840		-153.8314967117	
NCN	-146.7543056438	-146.7550570760	-146.7960367241	-146.7969897471
	-146.7538252278		-146.7960929213	
	-146.7538570945		-146.7960098936	
	-146.7538572568		-146.7959410054	
	-146.7539947678		-146.7960161292	

Table S7. (continued)

System	E(Singlet)/Hartree		E(Triplet)/Hartree	
	BPE	CAS-CI	BPE	CAS-CI
CNN	-146.6981008702	-146.6988098744	-146.7354381598	-146.7364385327
	-146.6974183633			
	-146.6972770350			
	-146.6978890615			
	-146.6972176034			
		-146.7355161053		
		-146.7354771912		
		-146.7354702073		
		-146.7352579209		

Table S8. Vertical excitation energies computed by using BPE, BPDE, and CAS-CI methods.

System	Excited state	Excitation energy/eV			
		BPE	BPDE	CAS-CI	Exptl.
CF ₂	1 ¹ B ₁	6.2032	6.1958	6.1428	4.614 ^[S12]
		6.2017	6.1989		
		6.1974	6.2008		
		6.1989	6.1998		
		6.2001	6.1988		
	1 ³ B ₁	3.0617	3.0612	2.9991	2.458 ^[S12]
		3.0641	3.0624		
		3.0577	3.0624		
		3.0573	3.0635		
		3.0608	3.0618		
CCl ₂	1 ¹ B ₁	3.1906	3.1860	3.1913	2.139 ^[S12]
		3.1864	3.1871		
		3.1874	3.1859		
		3.1872	3.1855		
		3.1908	3.1868		
	1 ³ B ₁	1.3610	1.3624	1.3599	0.9(2) ^[S13]
		1.3508	1.3642		
		1.3513	1.3610		
		1.3564	1.3618		
		1.3527	1.3613		
CBr ₂	1 ¹ B ₁	2.7467	2.7454	2.7551	1.871 ^[S12]
		2.7435	2.7472		
		2.7458	2.7484		
		2.7447	2.7479		
		2.7466	2.7464		
	1 ³ B ₁	1.2055	1.2101	1.2185	Not available
		1.2023	1.2070		
		1.2028	1.2082		
		1.2063	1.2071		
		1.2071	1.2069		

Table S8. (continued)

System	Excited state	Excitation energy/eV			
		BPE	BPDE	CAS-CI	Exptl.
SiF ₂	1 ¹ B ₁	6.6209	6.6220	6.6425	5.469 ^[S12]
		6.6245	6.6214		
		6.6215	6.6218		
		6.6227	6.6216		
		6.6217	6.6234		
	1 ³ B ₁	3.6358	3.6497	3.6629	3.262 ^[S12]
		3.6415	3.6512		
		3.6394	3.6505		
		3.6402	3.6523		
		3.6388	3.6502		
SiCl ₂	1 ¹ B ₁	4.6906	4.6863	4.6894	3.721 ^[S12]
		4.6863	4.6871		
		4.6894	4.6850		
		4.6900	4.6861		
		4.6864	4.6868		
	1 ³ B ₁	2.6396	2.6364	2.6393	2.349 ^[S12]
		2.6393	2.6376		
		2.6415	2.6387		
		2.6411	2.6394		
		2.6381	2.6373		
HCHO	1 ¹ A ₂	5.2923	5.2979	5.3586	4.1 ^[S14]
		5.3000	5.2970		
		5.2930	5.2988		
		5.2866	5.2961		
		5.2893	5.2973		
	1 ¹ B ₁	10.4590	10.4662	10.5254	8.6–9.0 ^[S15]
		10.4653	10.4664		
		10.4741	10.4660		
		10.4648	10.4666		
		10.4717	10.4672		

Table S8. (continued)

System	Excited state	Excitation energy/eV			
		BPE	BPDE	CAS-CI	Exptl.
HCHO	$2\ ^1A_1$	11.5963	11.6041	11.6920	10.7 ^[S14]
		11.5809	11.6029		
		11.5867	11.6028		
		11.5852	11.6036		
		11.5801	11.6031		

Table S9. Total energies of the electronic ground and excited states calculated by using BPE and CAS-CI methods.

System	Electronic state	E(BPE)/Hartree	E(CAS-CI)/Hartree
CF ₂	1 ¹ A ₁	-236.6710204355	-236.6710458231
		-236.6710092140	
		-236.6708698350	
		-236.6708316210	
		-236.6709286526	
	1 ¹ B ₁	-236.4430589779	-236.4453026215
		-236.4431021834	
		-236.4431213697	
		-236.4430274993	
		-236.4430783931	
	1 ³ B ₁	-236.5585054552	-236.5608284940
		-236.5584072246	
		-236.5585030805	
		-236.5584771860	
		-236.5584472161	
CCl ₂	1 ¹ A ₁	-956.7190349863	-956.7191074862
		-956.7189806638	
		-956.7189382279	
		-956.7189954401	
		-956.7190179626	
	1 ¹ B ₁	-956.6017826830	-956.6018257243
		-956.6018818945	
		-956.6018021249	
		-956.6018667680	
		-956.6017586717	
	1 ³ B ₁	-956.6690207713	-956.6691305743
		-956.6693407989	
		-956.6692802186	
		-956.6691486617	
		-956.6693056282	

Table S9. (continued)

System	Electronic state	E(BPE)/Hartree	E(CAS-CI)/Hartree
CBr ₂	1 ¹ A ₁	-5181.9600564926	-5181.9601544990
		-5181.9600050278	
		-5181.9599774488	
		-5181.9600219865	
		-5181.9600718438	
	1 ¹ B ₁	-5181.8591163864	-5181.8589047770
		-5181.8591837900	
		-5181.8590719284	
		-5181.8591575827	
		-5181.8591366835	
	1 ³ B ₁	-5181.9157534003	-5181.9153748136
		-5181.9158195543	
		-5181.9157747571	
		-5181.9156929067	
		-5181.9157132716	
SiF ₂	1 ¹ A ₁	-487.8864044197	-487.8899389221
		-487.8865311964	
		-487.8865188036	
		-487.8865166428	
		-487.8864687027	
	1 ¹ B ₁	-487.6430917474	-487.6458314455
		-487.6430862702	
		-487.6431832597	
		-487.6431352970	
		-487.6431275530	
	1 ³ B ₁	-487.7527910427	-487.7553299187
		-487.7527102921	
		-487.7527747177	
		-487.7527407951	
		-487.7527454888	

Table S9. (continued)

System	Electronic state	E(BPE)/Hartree	E(CAS-CI)/Hartree
SiCl ₂	1 ¹ A ₁	-1207.9510148766	-1207.9509641610
		-1207.9509397647	
		-1207.9509991770	
		-1207.9510312737	
		-1207.9509091348	
	1 ¹ B ₁	-1207.7786396268	-1207.7786311184
		-1207.7787207980	
		-1207.7786665136	
		-1207.7786784011	
		-1207.7786880525	
	1 ³ B ₁	-1207.8540113542	-1207.8539704120
		-1207.8539462435	
		-1207.8539265730	
		-1207.8539736750	
		-1207.8539625317	
HCHO	1 ¹ A ₁	-113.8938923458	-113.8968576086
		-113.8939198155	
		-113.8939558511	
		-113.8938866768	
		-113.8939462866	
	1 ¹ A ₂	-113.6994046925	-113.6999336744
		-113.6991481250	
		-113.6994406369	
		-113.6996076059	
		-113.6995694149	
	1 ¹ B ₁	-113.5095330911	-113.5100580837
		-113.5093268767	
		-113.5090410299	
		-113.5093108264	
		-113.5091201585	

Table S9. (continued)

System	Electronic state	E(BPE)/Hartree	E(CAS-CI)/Hartree
HCHO	$2\ ^1A_1$	-113.4677377190	-113.4671845004
		-113.4683311388	
		-113.4681512375	
		-113.4681395649	
		-113.4683851785	

7. Trotter decomposition error analysis

As discussed in the main text, ionisation energies of HF molecule and singlet–triplet energy gap of H₂ molecule with shorter atom–atom distances ($R(\text{H}\cdots\text{H}) \leq 1.5 \text{ \AA}$) computed by using BPDE algorithm exhibit considerably large deviations from the CAS-CI values. In order to disclose the origin of this error, we examined numerical quantum circuit simulations with different number of Trotter slices. We also examined the numerical simulations with tighter threshold for convergence. The simulation results discussed in the main text uses the convergence threshold $E_{\text{thre}} = 0.005$ Hartree, but here we used $E_{\text{thre}} = 0.001$ Hartree.

Results of the quantum circuit simulations of HF and H₂ are summarised in Fig. S17 and 18, respectively. Deviation from the CAS-CI value becomes smaller by shortening the time for single Trotter steps (t/N). Similar trend was also observed in the ionisation energy calculations using the BxB algorithm.^[S2] The calculated ionisation energy of HF does not depend on the energy threshold for convergence, but in the singlet–triplet energy gap of H₂ tighter threshold gives smaller deviation from the full-CI value, except for $R(\text{H}\cdots\text{H}) = 1.2 \text{ \AA}$ with $t/N = 0.5$. We conclude that the Trotter decomposition error is mainly responsible for the deviation of the energy gaps from the CAS-CI values.

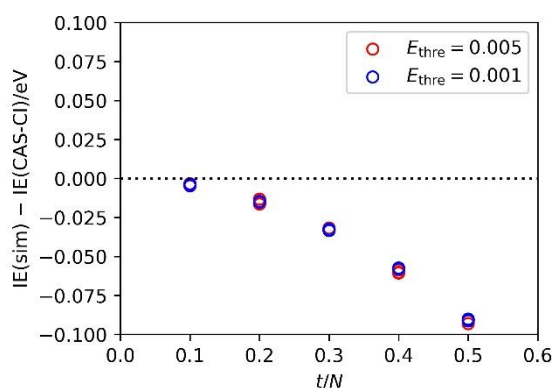


Fig. S17 Deviations between the vertical ionisation energies obtained from the numerical quantum circuit simulations of BPDE algorithm and CAS-CI calculations in HF molecule with the different single Trotter step lengths t/N from 0.1 to 0.5 atomic unit.

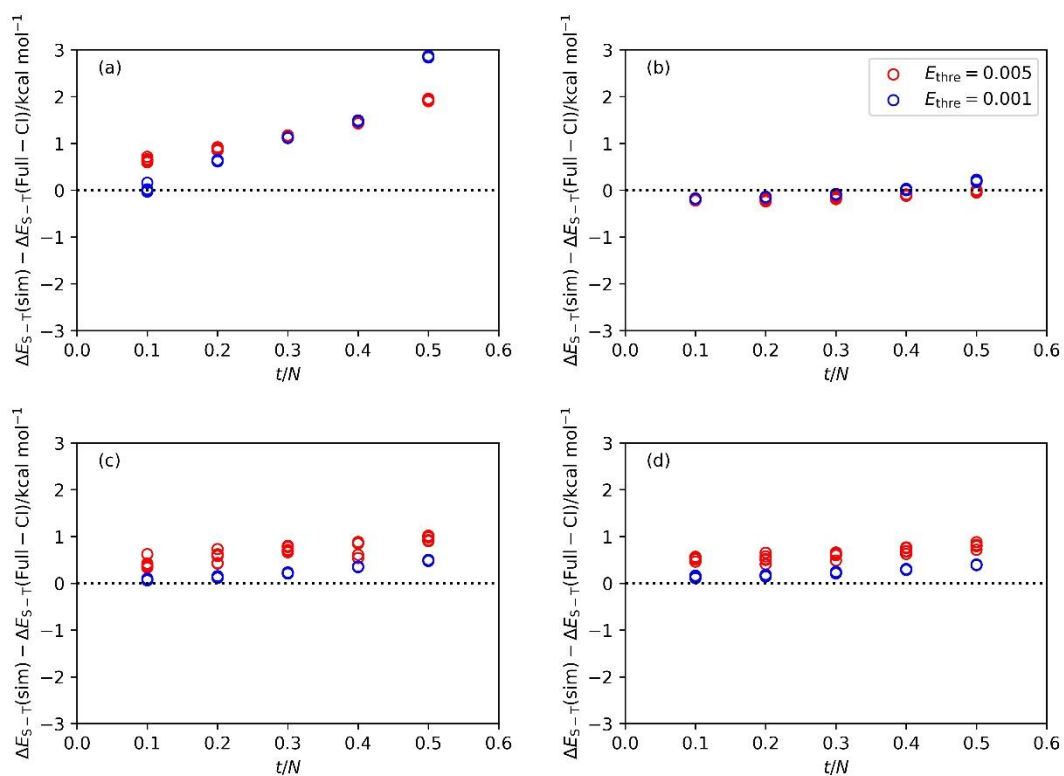


Fig. S18 Deviations between the singlet–triplet energy gaps of H₂ molecule obtained from the numerical quantum circuit simulations of BPDE algorithm and CAS-CI calculations with the different single Trotter step lengths t/N from 0.1 to 0.5 atomic unit. (a) $R(\text{H}\cdots\text{H}) = 1.2 \text{ \AA}$, (b) $R(\text{H}\cdots\text{H}) = 1.3 \text{ \AA}$, (c) $R(\text{H}\cdots\text{H}) = 1.4 \text{ \AA}$, (d) $R(\text{H}\cdots\text{H}) = 1.5 \text{ \AA}$

8. References

- [S1] M. J. Frisch, et al. *Gaussian 09, revision B.01*, Gaussian Inc., Wallingford, CT, 2009.
- [S2] K. Sugisaki, K. Toyota, K. Sato, D. Shiomi and T. Takui, Quantum algorithm for the direct calculations of vertical ionization energies, *J. Phys. Chem. Lett.*, 2021, **12**, 2880–2885.
- [S3] M. W. Schmidt, et al. General atomic and molecular electronic structure system, *J. Comp. Chem.*, 1993, **14**, 1347–1363.
- [S4] A. Tranter, P. J. Love, F. Mintert and P. V. Coveney, A comparison of the Bravyi–Kitaev and Jordan–Wigner transformations for the quantum simulation of quantum chemistry, *J. Chem. Theory Comput.*, 2018, **14**, 5617–5630.
- [S5] A. Tranter, P. J. Love, F. Mintert, N. Wiebe and P. V. Coveney, Ordering of Trotterization: Impact on errors in quantum simulation of electronic structure, *Entropy*, 2019, **21**, 1218.
- [S6] W. C. Martin, A. Musgrove, S. Kotochigova and J. E. Sansonetti, Ground levels and ionization energies for the neutral atoms, *NIST Standard Reference Database III*. **2013**, DOI: 10.18434/T42P4C
- [S7] S. G. Lias, Ionization energy evaluation, In *NIST Chemistry WebBook, NIST Standard Reference Database Number 69*, ed, P. J. Linstrom and W. G. Mallard, National Institute of Standards and Technology, DOI: 10.18434/T4D303 (retrieved January 11, 2021).
- [S8] A. R. Striganov and N. S. Sventitskii, *Tables of Spectral Lines of Neutral and Ionized Atoms*. Springer, New York, 1968.
- [S9] K. P. Huber and G. Herzberg, *Molecular Spectra and Molecular Structure IV. Constants of Diatomic Molecules*. Springer, New York, 1979.
- [S10] T. R. Taylor, R. T. Bise, K. R. Asmis and D. M. Neumark, The singlet–triplet splittings of NCN, *Chem. Phys. Lett.*, 1999, **301**, 413–416.
- [S11] E. P. Clifford, P. G. Wenthold, W. C. Lineberger, G. A. Petersson, K. M. Broadus, S. R. Kass, S. Kato, C. H. DePuy, V. M. Bierbaum and G. B. Ellison, Properties of diazocarbene [CNN] and the diazomethyl radical [HCNN] via ion chemistry and spectroscopy, *J. Phys. Chem. A*, 1998, **102**, 7100–7112.
- [S12] M. E. Jacox, Vibrational and electronic energy levels of polyatomic transient molecules. *J. Phys. Chem. Ref. Data, Monograph 3*, 1994.
- [S13] S. W. Wren, K. M. Vogelhuber, K. M. Ervin and W. C. Lineberger, The photoelectron spectrum of CCl₂⁻: the convergence of theory and experiment after a decade of debate, *Phys. Chem. Chem. Phys.*, 2009, **11**, 4745–4753.
- [S14] L. B. Harding and W. A. Goddard, Ab initio theoretical studies of the Rydberg states of formaldehyde, *J. Am. Chem. Soc.*, 1977, **99**, 677–683.
- [S15] D. C. Moule and A. D. Walsh, Ultraviolet spectra and excited states of formaldehyde, *Chem. Rev.*, 1975, **75**, 67–84.